Annals of Biomedical Engineering, Vol. 31, pp. 310–317, 2003
Printed in the USA. All rights reserved.

0090-6964/2003/31(3)/310/8/$20.00

Modeling the Dynamic Characteristics of Pneumatic Muscle

D. B. REYNOLDS,[1] D. W. REPPERGER,[2] C. A. PHILLIPS,[1] and G. BANDRY[1]

[1]Department of Biomedical, Industrial and Human Factors Engineering, Wright State University, Dayton, OH and [2]AFRL/HECP, Wright-Patterson Air Force Base, Dayton, OH

(Received 24 July 2002; accepted 3 January 2003)

Abstract—A pneumatic muscle (PM) system was studied to determine whether a three-element model could describe its dynamics. As far as the authors are aware, this model has not been used to describe the dynamics of PM. A new phenomenological model consists of a contractile (force-generating) element, spring element, and damping element in parallel. The PM system was investigated using an apparatus that allowed precise and accurate actuation pressure (P) control by a linear servovalve. Length change of the PM was measured by a linear potentiometer. Spring and damping element functions of P were determined by a static perturbation method at several constant P values. These results indicate that at constant P, PM behaves as a spring and damper in parallel. The contractile element function of P was determined by the response to a step input in P, using values of spring and damping elements from the perturbation study. The study showed that the resulting coefficient functions of the three-element model describe the dynamic response to the step input of P accurately, indicating that the static perturbation results can be applied to the dynamic case. This model is further validated by accurately predicting the contraction response to a triangular P waveform. All three elements have pressure-dependent coefficients for pressure P in the range $207 \leqslant P \leqslant 621$ kPa ($30 \leqslant P \leqslant 90$ psi). Studies with a step decrease in P (relaxation of the PM) indicate that the damping element coefficient is smaller during relaxation than contraction. © *2003 Biomedical Engineering Society.* [DOI: 10.1114/1.1554921]

Keywords—Artificial muscle, McKibben muscle, Pneumatic actuator.

INTRODUCTION

A pneumatic muscle (PM) is an interesting actuator (very similar in action to animal skeletal muscle), which has two significantly important advantages.[3,12–15]

(1) It has a power/weight ratio of 1 W/g.
(2) It has a power/volume ratio of 1 W/cm^3.

Both these ratios are about five times higher in comparison to an electric motor or a hydraulic actuator. Of course, a gas supply must be included in the total PM system, so this must be factored in when comparing system performance. Pneumatic actuator systems have applications in robotics, including dextrous manipulators,[3] in physical therapy for functional recovery therapy[10] and for strength augmentation devices involving humans which have to be self-contained and carried long distances.[12] Originally, pneumatic muscle was developed as an actuator for a human arm orthosis.[17] Pneumatic muscles work similarly to the manner that human or animal muscle acts (a force or moment is only created through the action of a contraction). Recently, Phillips and co-workers[11] have formulated a posture control strategy for a human exoskeleton having PMs at the thigh and hip. In this model, one-dimensional contraction of the PMs results in two-dimensional motion of the exoskeleton.

Another advantage of the pneumatic muscle system technology is in its ability to perform like a ''soft actuator.''[3] In the robotics literature, this refers to the property that in the event of structural failure, the human (if proximal to the force generating system) is at a very low level of risk of injury. This is not the case for hydraulic and/or electric motor actuators, which, when failing, produce a far greater risk of injury to the human user adjacent to the device.

The main problem with pneumatic actuators, including pneumatic muscle actuators, is their inaccurate and difficult control. This is mainly due to their high compliance resulting from the compressibility of the gas.[3,4] In case of pneumatic muscle, the nonlinear elasticity of the bladder contained within the braided sheath and the mechanical characteristics of the bladder/sheath combination under pressure are additional considerations. The methods of classical control require a model of the system in order to design a controller. This paper considers a new, simple model for a pneumatic muscle, which can be used to aid in the development of control systems, so that pneumatic muscle actuators may better perform their intended function in industrial robots as well as in prosthetic, orthotic, and other human-assistive systems.

Address correspondence to D. B. Reynolds, Dept. BIE, 207 Russ Engineering Center, Wright State University, Dayton, OH 45435. Electronic mail: david.reynolds@wright.edu

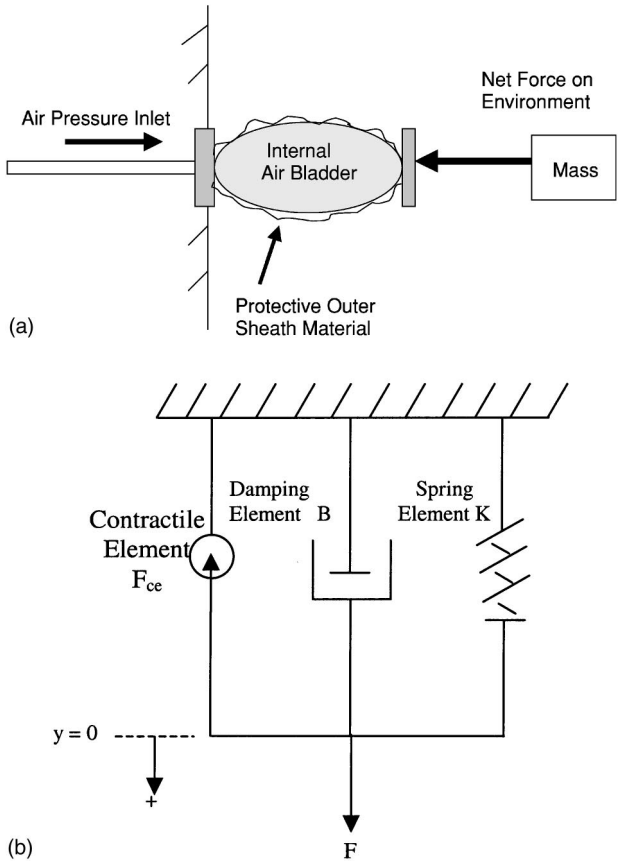

FIGURE 1. (a) Schematic drawing of the pneumatic muscle, (b) three-element model of pneumatic muscle.

PRINCIPAL OF OPERATION OF A PNEUMATIC MUSCLE

The basic principle of operation of a PM system incorporates a thin-walled, rubber bladder (compliant material) placed inside an axially stiff but radially compliant braided sheath, as shown schematically in Fig. 1(a). As the rubber bladder expands due to an increase in pressure, the diameter of the combined sheath and bladder assembly easily changes in the radial direction and the muscle shortens in the axial direction. Thus, the force exerted on the environment occurs in the axial direction. As a consequence of this interaction, the large contractive force produced can perform external work at a rapid rate (high power). However, nonlinearities exist as the pressure changes in the bladder because its area expands proportionally to the square of the diameter. Also as the outer sheath material moves, its length is dependent on trigonometric relationships involving the outer sheath material, which are nonlinear. Chou and Hannaford[5] and Caldwell[4] give theoretical estimates of the net force produced on the environment.

BACKGROUND

Pneumatic muscle actuator, or McKibben pneumatic artificial muscle as it is sometimes termed, was developed in the 1950's and early 1960's as part of an orthotic limb system. McKibben evidently did not publish his original work, but has been quoted by Baldwin[1] as having derived equations relating contracted length and contractile force to internal pressure for a PM having axially arranged fibers. Baldwin extends the theory attributed to McKibben for nonzero tube diameters.[1]

Designs using double-helically wound fibers as the shell around the inner bladder became more popular in the 1960's, even though Baldwin claims that the axial tension fibers may have higher mechanical efficiency.[1] Schulte appears to be the first to analyze force produced by pressure with the helically wound PM[16] and others have essentially obtained similar results.[4,5] The most complex of these equations relates the contractile force to the pressure, the diameter of the PM when the helical fibers are perpendicular to the tube axis, the thickness of the combined shell and bladder, and the trigonometric functions of the helix angle with respect to the axial direction.[5] This type of equation is suitable for mechanical design of a PM, but because the equation parameters cannot be measured during actuation, it does not help to model the system for the purpose of actuator control, which is necessary for classical nonlinear control.

Problems with control of PM seem to have resulted in a nearly 30 year hiatus in PM research, finally ending with research by Inoue[8] and Caldwell.[2] Caldwell attributes this difficulty in control to the interrelated problems of lack of accuracy of position control and air compliance, which causes position change with load variation.[3] The latter drawback and the need for a compressed air supply also led to abandonment of PM for prosthetic and orthotic applications.[3,7]

Inoue discusses the use of a braided pneumatic actuators developed by Bridgestone for applications to robotics.[8] His apparatus uses an agonist/antagonist pair (borrowing the terminology from skeletal muscle physiology) of actuators connected by a wire rope over a pulley. He does suggest a second order model for the rotation angle of the pulley, with the forcing function proportional to the pressure difference between that supplied to the actuator pair.[8] In this model, there is a frictional term proportional to the angular velocity of the pulley and a spring term proportional to the pulley angle. The latter term allows open loop position control, which is not available for motor or gas cylinder servo systems.[8] No explicit relationships between the friction or spring coefficients and pressure are given, although Inoue does give a relationship between contraction force and pressure, which has been used by others.[17] The interesting aspect of Inoue's study is that it uses pressure difference

between the PM pair rather than pressure for a single PM.

Winters[18] and Hannaford and Winters[7] describe renewed interest in prosthetic applications using PMs. Chou and Hannaford[5] describe static and dynamic characteristics of braided PM and modeling of the pneumatic circuit dynamics. However, no phenomenological model of the dynamic behavior of PM was proposed.

In this paper, we describe a new phenomenological model for the dynamics of a PM actuator. The model is a parallel arrangement of a spring element, damping element, and contractile force element. Each element has a coefficient that is a function of the actuation pressure.

THEORY

Model of the Pneumatic Muscle

The model is shown in Fig. 1(b), which is a parallel arrangement of a spring element, damping element and contractile element, an adaptation of the Voight viscoelastic model.[6] In this paper, expressions for the coefficients of the elements as functions of the independent variable of interest, pressure (P), are determined experimentally. This model differs from Hill's model of skeletal muscle in that it has a single parallel spring rather than springs in series and parallel.[6]

Letting y be position, the equations of motion for the system studied become

$$M\ddot{y}+B\dot{y}+Ky=F_{ce}-Mg, \tag{1}$$

where K is the spring coefficient, B is the damping coefficient, and F_{ce} is the effective force provided by the contractile element. For the experimental configuration presented here, the external force F in Fig. 1(b) is the load due to the weight (Mg) plus the inertial load ($M\ddot{y}$). All mass in the system is assumed to be in the vertically oriented mass of the load M. Note that when $Mg=F_{ce}$ and zero initial displacement and velocity $[y(0)=\dot{y}(0)=0]$, no motion occurs. For loads less than this, $F_{ce}>Mg$ and the right-hand side of Eq. (1) becomes the driving function for the system studied.

The contractile force F_{ce} also depends on geometric factors of the sheath as well as the thickness of the sheath/bladder combination, as given by Chou and Hannaford.[5] Other theoretical approaches ignore bladder elasticity in predicting the length of the PM during contraction.[1] Recently, Klute and Hannaford[9] have included bladder elasticity in a theory for the output force of a PM.

At a steady state P, and thus constant F_{ce}, the PM is further modeled as a spring element and damping element in parallel, or Voight model.[6] We further hypothesize that the spring and damping coefficient functions determined by perturbating the load at constant P are the same functions as pertain to the dynamic condition.

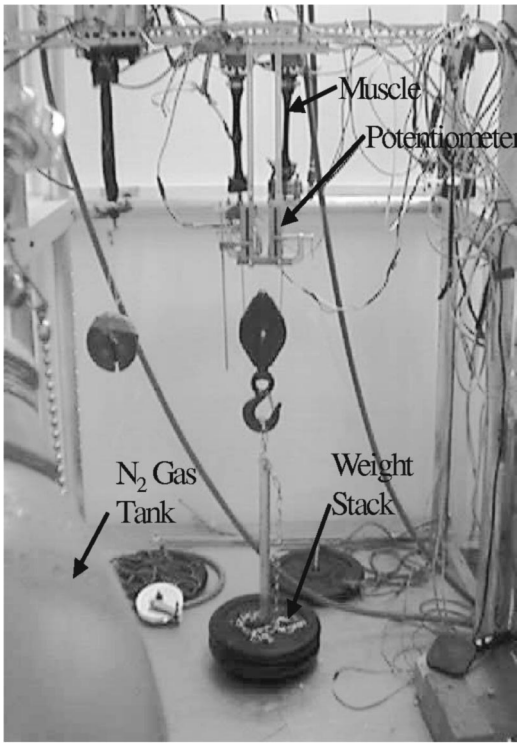

FIGURE 2. Experimental apparatus, showing both of the PMs reported on in this study. Stretched length of the PM between the hose clamps is about 150 mm. While the two PMs on the right are shown as an agonist-antagonist pair, only one at a time was studied. The load cells are visible both above and below the PM. Also visible are the linear servovalves above the PM at the far left. The pressure transducers are also at the very top of the picture, just above the horizontal support beam. The 25 lb weights are standard barbell devices found in gyms.

METHODS

Pneumatic Muscle (PM)

Two nearly identical PMs were constructed of an inner bladder made from a section of 22.2 mm (7/8 in.) diameter bicycle tire tubing (size 27-s-143) enclosed in a nylon sheath used for supporting electrical cables (Astro Industries, Inc., Dayton OH, Cat. No. SCGRP-120-1250-0) The unstretched, uncompressed diameter of the sheath is 31.75 mm (1.25 in.). One end was hose-clamped to an adapter made in-house, which held a tubular connector to a proportional control valve (Festo Corp., Hauppauge, NY, model MPPE-3-1/8-10-010B). The valve was connected to a regulated N_2 gas pressure source. The other end of the PM, hose-clamped to a closed-off adapter, was attached to a weight stack as depicted in Fig. 2. Note that due to the 2:1 transmission of the pulley, the load on the PM is the pulley system

plus stack weight divided by 2. The tubular connector was constructed from a 9.50 mm (3/8 in.) bolt with a 4.75 mm (3/16 in.) hole drilled down the center. The no-load length of the PM is about 140 mm (5.5 in.) between adapters and its weight without adapters is 0.059 kg (0.13 lb).

Experimental Apparatus and Data Collection

The PM was oriented vertically in a clear plastic chamber, as shown in Fig. 2. A variable weight stack was hung via pulley, hook and chains directly below the PM. Another PM placed in parallel around the pulley, which could be used as an antagonist PM, is shown in Fig. 2 but was not pressurized and thus was only passive in this study. However, the other PM shown in Fig. 2 was used singly in a similar set of experiments, whose results are reported here, in which the former PM was passive. The pulley, hook, and supporting apparatus weighed 26.7 N (6 lb).

The length change of the muscle was measured by a low friction linear potentiometer (Duncan Electronics Inc., Costa Mesa CA, 50 kΩ Slideline) attached to the moving lower end of the PM. The top of the PM (with the gas inlet connector) was fixed to a horizontal support beam.

A pressure transducer (Omega Engineering, model PX906-500-GV, 0-500 psi) measured inlet pressure to the PM, and was positioned about 150 mm (6 in.) upstream of the inlet. Load cells (A.L. Design Inc., model ALD-DLC, 250 lb) placed just above and below the PM measured load, which can also be determined by half the weight on the stack and pulley system, as mentioned earlier.

Data were collected using a multichannel PC-based data acquisition system. The procedure was programed to open the servovalve to the regulated gas supply, providing a step increase in pressure to the PM (servovalve time constant of 0.3 s). A data run consisted of 800 points per channel, thus, at a 64 Hz sampling frequency, 12.5 s of data were collected.

Pressures in the range of 207–621 kPa (30–90 psi) and loads in the range of 57.8–898 N (13–201.8 lb) were studied. At lower pressure, the full range of load was not applied because the PM was limited in its ability to shorten.

RESULTS AND DISCUSSION

Perturbation ("Bell Ringer") Study

To provide independent estimates of B and K as functions of pressure, after pressure had reached a steady state we suddenly reduced the weight from a larger weight stack thus, the nickname bell ringer describing how a portion of the load was lifted by two technicians pulling simultaneously on ropes. This was accomplished for constant pressures of 207–621 kPa (30–90 psi) in steps of 68.9 kPa (10 psi). An example of the results at 414 kPa (60 psi) is depicted in Fig. 3. The first portion of the curve is due to the muscle contraction at 414 kPa for a load of 347 N (78 lb). At about 6 s, 111 N (25 lb) was suddenly removed and the muscle contracted an additional 5.6 mm. Note that this represents the length change with variation in load referred to by Caldwell[3] earlier. A 347 N load was chosen because it is a representative load, about half of the maximum load capable of being lifted by the PM. The suddenly removed load is about a third of initial load. The time to remove the weight was estimated from load cell data and was less than 0.1 s in all cases, or about a third of the time constant of the resulting length change. Because there is no immediate displacement of the PM resulting from the load reduction nor is there a change in the contractile force F_{ce} because pressure is held constant, the length change after partial load removal is appropriately modeled by spring and damping elements in parallel, as mentioned earlier. The spring and damping coefficients K and B, respectively, are determined by fitting the data to the Voight model. This experiment was repeated three times at each pressure. The results are shown in Figs. 4 and 5. Both K and B increase linearly with pressure, but the results for B are more variable, with a smaller correlation coefficient 0.733 compared to 0.971 for K. However, each fit is significant at the 0.01 level. The variability in B is probably due to the experimental procedure, since B depends entirely on the transient portion of the curve, while K depends mainly on the removed load and resulting displacement of the muscle. The oscillation due to some bouncing of the remaining load is likely the source of the scatter in B, especially apparent

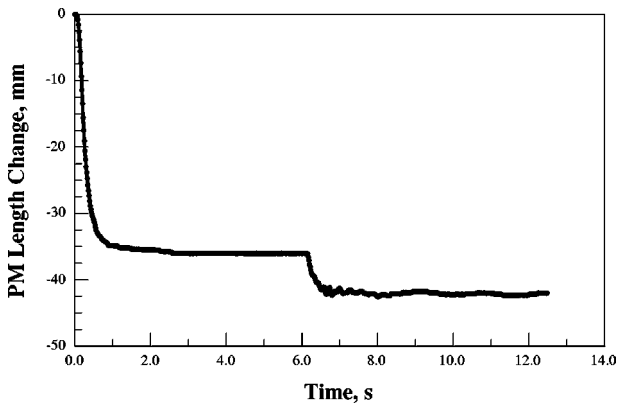

FIGURE 3. Shortening of PM at a pressure of 414 kPa (60 psi) and a load of 347 N (78 lb) is shown for 6 s. After that, 111 N (25 lb) was suddenly removed, giving the additional contraction shown. A small resonance of about 5 Hz is noted during the second contraction due to structural frame dynamics.

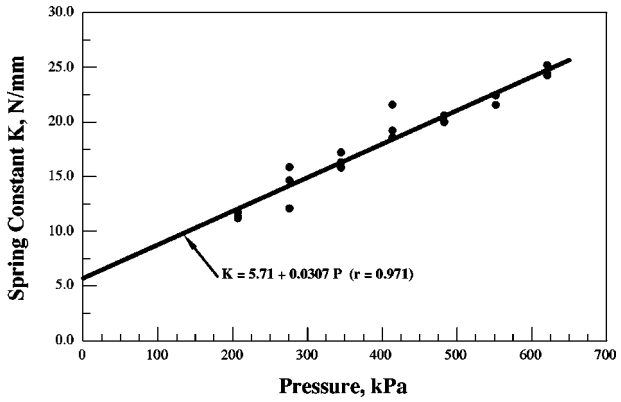

FIGURE 4. Spring constant *K* exemplified from sudden removal of load from the PM is shown vs. the pressure.

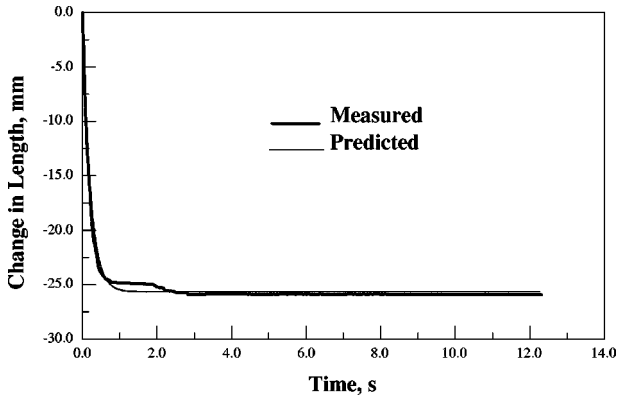

FIGURE 6. Time history of contraction for a step input in pressure of 483 kPa (70 psi) with a 347 N (78 lb) load. Also shown is prediction using the overdamped solution of the three-element model, with parameters *K* and *B* determined from the perturbation study. Only F_{ce} was found by a least squares fit to the time history.

at 550 kPa (80 psi) in Fig. 5. That *B* and *K* could be functions of the load and removed load is possible as well. As shown in the next section, that a three-element model, with *K* and *B* dependent only on pressure, closely predicts the transient portion of the entire step response to pressure indicates that this effect is not significant.

Contraction Study: Step Response to Pressure

Additional contraction studies were accomplished at 207, 345, 483, and 621 kPa (30, 50, 70, and 90 psi) with loads of 57.8, 80.1, 125, 169, 236, 347, 458, 570, 681, 792, and 899 N (13, 18, 28, 38, 53, 78, 103, 128, 153, 178, and 202 lb). Loads of 57.8 and 80.1 N were only used for one of the two muscles at 207 kPa and some of the heavier loads could only be lifted at the higher pressures.

A typical example of contraction for one of the two muscles studied at 483 kPa (70 psi) for a load of 347 N (78 lb) is shown in Fig. 6. The curves are similar in shape and magnitude, as expected. There was a time delay before the contraction started and all curves were analyzed after this delay. This delay was determined from the sampled data as the time between the initial rise of the pressure step as measured by the pressure transducer and the initial movement of the PM as measured by the potentiometer. The delay increased with applied load and decreased with pressure and averaged 0.23 $\pm$0.185 s for all data collected for the two PMs studied. This delay has been noted in the literature, attributed to Coulomb or static friction (''stiction'') between the sheath and bladder. This stiction could be reduced by the addition small tremor signal (dither).

The contraction curves were fit to the overdamped solution of the length change of the model for a step increase in pressure. The *K* and *B* from the bell-ringer or perturbation study described in the last section were used so that the only parameter determined from the curve fit is the contractile force F_{ce}. Note that F_{ce} so determined does not depend on the transient portion of the contraction curve but only on the steady state portion.

The estimated F_{ce} for the two similar but independently tested muscles at the several loads is illustrated in Fig. 7. Horizontal lines shown represent mean values at a given pressure. Although the difference between the results for the two PMs is readily apparent at 621 kPa (90 psi) for loads less than 681 N (153 lb), at lower pressures the results are practically coincident and difficult to distinguish on the figure. The estimated values do not vary appreciably with the load, but increase with pressure. Except for the results at 621 kPa (90 psi), the two muscles have nearly equal F_{ce} at a given pressure. There is a tendency for the estimated F_{ce} to increase slightly with load, however, the maximum variation from the mean F_{ce} is only 10%–15%. Note that the highest

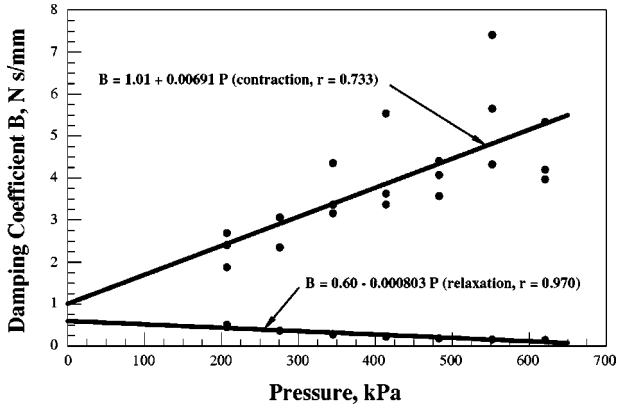

FIGURE 5. Damping coefficient *B* exemplified from sudden removal of load is shown as the upper line. The lower line is *B* for relaxation studies.

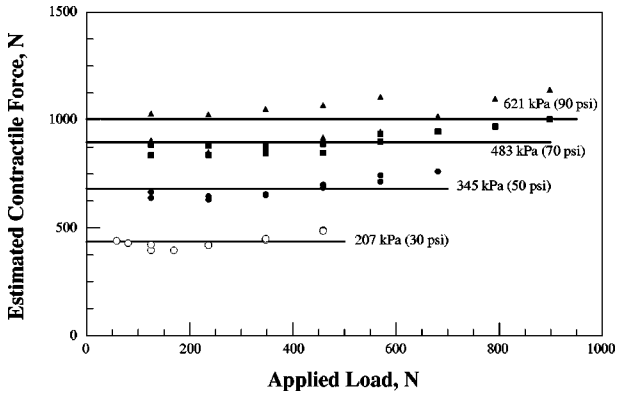

FIGURE 7. Contractile force F_{ce} at the several applied loads for the four pressures studied 207, 345, 483, and 621 kPa (30, 50, 70, and 90 psi) is computed from the model as the only remaining unknown parameter. Horizontal lines indicate mean values of F_{ce}.

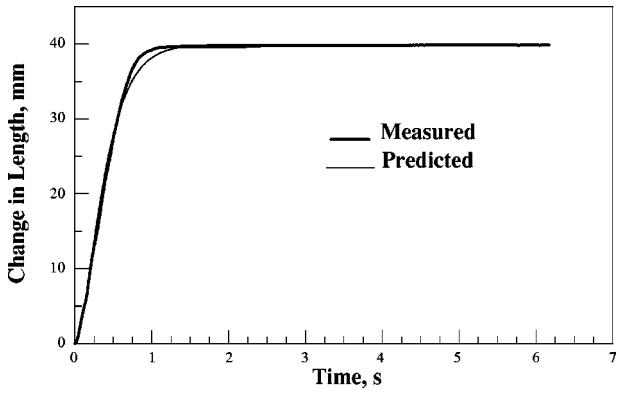

FIGURE 9. Time history of PM length increase during relaxation from an initial pressure of 345 kPa (50 psi). Load in all relaxation studies was 125 N (28 lb). Also shown is the three-element model prediction for the critically damped solution.

applied loads are close to the estimated F_{ce} so that the lines representing the mean values require essentially no extrapolation to higher load.

Mean F_{ce} values from Fig. 7 as a function of pressure is portrayed in Fig. 8. The linear fit has a correlation coefficient $r=0.986$, with significance of the fit at the 0.01 level. It should be emphasized that this relation between F_{ce} and P is only valid over the range $207 \leqslant P \leqslant 621$ kPa ($30 \leqslant P \leqslant 90$ psi). The curve for a theoretical maximal force evaluated from Eq. (10) in Chou and Hannaford[5] applied to our PM geometry (45.7 mm sheath diameter at 90° braid angle and 1.37 mm sheath/bladder thickness) is also shown in this figure.

The two curves give similar values for F_{ce} at 207 kPa (30 psi), where our results intersect the theoretical curve. However, at 621 kPa (90 psi), our results are 30% lower than the theoretical value.

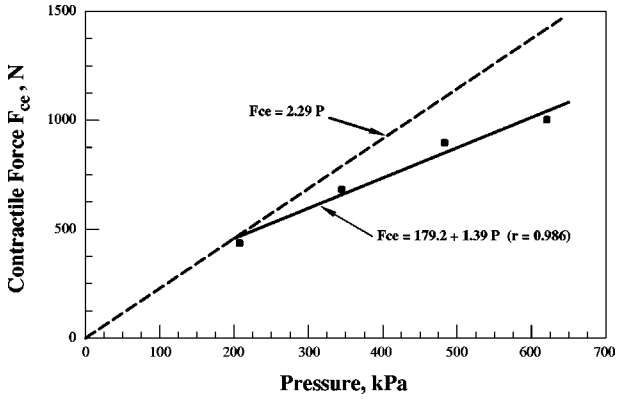

FIGURE 8. Mean contractile force F_{ce} from Fig. 7 is shown as a function of pressure. The dashed line is a theoretical estimate from an equation given in Ref. 5 applied to the PM used in this study.

Relaxation Study

Practically, relaxation is important since it completes the work loop of the activation cycle (contraction and relaxation). The dynamics of relaxation are just as important as contraction, since the net work produced on the environment requires both contraction and relaxation characteristics.

Relaxation (deflation) of a contracted PM was measured in the same apparatus at pressures from 207 to 621 kPa (30 to 90 psi) in increments of 68.95 kPa (10 psi). In all these experiments, a constant load of 125 N (28 lb) was applied and the PM was allowed to deflate from a steady contracted state to a fully relaxed state through a separate pneumatic line connected to atmosphere. The pressure decrease was achieved by suddenly opening the servovalve to atmosphere, resulting in a nearly step decrease in pressure and modeled in this manner.

A typical example of a relaxation length time history from a pressure of 345 kPa (50 psi) is shown in Fig. 9. One immediately observes that the curve changes more quickly than the corresponding contraction length curve (Fig. 6) and has an almost linear initial portion of the curve. Unlike the overdamped case for contraction, the relaxation curve is close to being critically damped, which explains the initial nearly linear portion of the curve. Using the critically damped solution to Eq. (1), with estimates of $K(P)$ from the bell ringer study in Fig. 4 ($r=0.971$) and $F_{ce}(P)$ from the contraction study in Fig. 8 ($r=0.986$), the relaxation damping coefficient $B(P)$ was found by a least-squares fit as indicated in Fig. 5 ($r=0.970$). For parsimony in the number of adjustable coefficients describing the dynamics of PM, only $B(P)$ was reanalyzed for relaxation.

Over the range of pressure studied, B for relaxation decreases with increasing pressure. As expected from the length relaxation curve, the value of B for relaxation is

21% of the B found for contraction at 207 kPa (30 psi), decreasing to 3% of the B for contraction at 621 kPa (90 psi).

Model Validation

Model prediction of the contraction length change to a step increase in pressure is shown in Fig. 6. The three-element model describes the experimental data with high accuracy. One might argue that it should because these data were used to find the coefficients of the model. However, the $K(P)$ and $B(P)$ were found by a step perturbation of the load while pressure was held constant. That these values of $K(P)$ and $B(P)$ also predict the entire transient portion of the contraction curve for all the pressures studied is not guaranteed and is an internal validation of the model. This finding also indicates that fluid friction in the inlet pneumatic line of our system did not contribute significantly to the overall damping, because the B coefficient was found using a perturbation method with essentially zero flow but it predicts the entire transient contraction curve for which there must have been flow to increase the PM volume.

Prediction of the length increase of the muscle back to the resting state during relaxation is shown in Fig. 9. The only parameter that is different from the contraction prediction in Fig. 6 is the damping coefficient B, which is considerably smaller for relaxation of the PM as shown in Fig. 5. Evidently there is less damping while the PM relaxes (deflates) than when it contracts (inflates). This may be for several reasons, including less friction between the outer sheath and the rubber bladder. The decrease in damping with increase in pressure during relaxation indicates a nonvelocity related friction, such as Coulomb friction mentioned by Chou and Hannaford.[5] The low value of this damping also indicates that friction in the exit pneumatic line is small, a conclusion we also draw for the inlet line in the prior paragraph.

External validation of the model is demonstrated in Fig. 10, which shows the experimental and predicted length change of PM to a triangular wave input of pressure between 55 and 124 kPa (8 and 18 psi) and frequency 0.17 Hz, also shown in Fig. 10. Simulations were computed using Simulink (MathWorks, Natick, MA). For ease of computation, we used $B(P)$ and $K(P)$ determined from the perturbation study, and applied these for both contraction and relaxation phases. At these lower pressures, F_{ce} was assumed to follow a quadratic fit of the data in Fig. 8 extrapolated to the origin. This fit would be very similar to the linear prediction of Chou and Hannaford[5] for pressure below 207 kPa (30 psi) shown in Fig. 8. The prediction has an rms error of 2 mm over a cycle or 15% of the average length change of the PM. The oscillations seen in the simulated length change result from similar oscillations in the experimental pressure waveform used as input to the simulation.

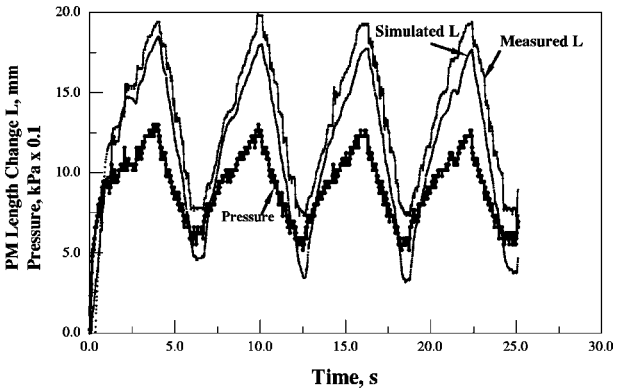

FIGURE 10. Simulated and measured length change of a PM with a triangular input pressure wave, which is also shown.

CONCLUSIONS AND RECOMMENDATIONS

The model shown in Fig. 1, with spring, dashpot, and contractile elements in parallel, appears to be an adequate phenomenological model to describe the motion of PM over a range of driving pressure between 207 and 621 kPa (30 and 90 psi) and loads up to the maximum that can be lifted. With our system, losses in the pneumatic lines seem to be negligible compared to damping within the PM itself. The accuracy of the model is demonstrated via the prediction curves in Figs. 6, 9, and 10.

Future work should include additional genuine replicates for improved statistical analysis. The effects of muscle length, both the initial length at which contraction starts for a given unstressed length and different unstressed lengths and diameters should be studied. Measurement of K and B at several loads and several load perturbations with pressure held constant should also be studied to verify nondependence of K and B on these parameters.

ACKNOWLEDGMENT

The authors would like to recognize the tireless efforts of Jim Berlin, without whose help these studies could not have been accomplished, and with whose help excellent data were obtained.

REFERENCES

[1] Baldwin, H. A. Muscle-like contractive devices. Bionics Symposium, Aeronautical Sys. Div./Aerospace Med. Div. Wright-Patterson AFB, 19–21 March 1963.

[2] Caldwell, D. G. Compliant polymeric actuators as robot drive units. PhD thesis, University of Hull, 1989.

[3] Caldwell, D. G., G. A. Medrano-Cerda, and M. Goodwin. Control of pneumatic muscle actuators. *IEEE Control Syst. Mag.* 2:40–48, 1995.
[4] Caldwell, D. G., N. Tsagarakis, and G. A. Medrano-Cerda. Bio-mimetic actuators: Polymeric pseudo muscular actuators and pneumatic muscle actuators for biological emulation. *Mechatronics* 10:499–530, 2000.
[5] Chou, C.-P., and B. Hannaford. Measurement and modeling of McKibben pneumatic artificial muscles. *IEEE Transactions on Robotics and Automation* 12:90–102, 1996.
[6] Fung, Y. C. Biomechanics: Mechanical Properties of Living Tissues, 2nd ed. New York: Springer, 1993, p. 568.
[7] Hannaford, B., and J. M. Winters. Actuator properties and movement control: Biological and technological models. In: Multiple Muscle Systems: Biomechanics and Movement Organization, edited by J. M. Winters and S. L.-Y. Woo. New York: Springer, 1990, pp. 101–120.
[8] Inoue, K. Rubbertuators and applications for robots. In: Robotics Research: The 4th International Symposium, edited by R. Bolles and B. Roth. Cambridge, MA: MIT Press, 1988, pp. 57–63.
[9] Klute, G. K., and B. Hannaford. Accounting for elastic energy storage in McKibben artificial muscle actuators. *Journal Dynamics Systems, Measurement, and Control* 122:386–388, 2000.
[10] Noritsuga, T., and T. Tanaka. Application of rubber artificial muscle manipulator as a rehabilitation robot. *IEEE/ASME Transactions on Mechatronics* 2:259–267, 1997.
[11] Phillips, C. A., D. W. Repperger, D. B. Reynolds, and G. Bandry. Posture control strategy for enhanced human performance exoskeletons. *Aviatation, Space, and Environmental Medicine* 73:296, 2002.
[12] Repperger, D. W. Strength augmentation system design for US Air Force missions. Proceedings of the DARPA Soldier Enhancement Workshop: Exoskeletons for Human Performance Augmentation, Session II, edited by E. Garcia, 23 September 1999, pp. 1–20.
[13] Repperger, D. W., K. R. Johnson, and C. A. Phillips. A VSC position tracking system involving a large scale pneumatic muscle actuator. Proceedings of the Conference on Decision and Control, Tampa, Florida, 16–18 Dec. 1998, pp. 4302–4307.
[14] Repperger, D. W., C. A. Phillips, D. C. Johnson, R. D. Harmon, and K. Johnson. A study of pneumatic muscle technology for possible assistance in mobility. Proceedings of the IEEE EMBS, Chicago, 30 Oct.–2 Nov. 1997, pp. 1884–1887.
[15] Repperger, D. W., C. A. Phillips, and M. Krier. Controller design involving gain scheduling for a large scale pneumatic muscle actuator. Proceedings of the Conference on Control Applications, Hawaii, 22–27 Aug. 1999, pp. 285–290.
[16] Schulte, H. F. The characteristics of the McKibben artificial muscle. In: The Application of External Power in Prosthetics and Orthotics. Washington, DC: Pub. 874, National Academy of Science-National Research Council, 1961, pp. 94–115.
[17] Tondu, B., and P. Lopez. The McKibben muscle and its use in actuating robot-arms showing similarities with human arm behavior. *Ind. Robot* 24:432–439, 1997.
[18] Winters, J. M. Braided artificial muscles: Mechanical properties and future uses in prosthetics/orthotics. 13th RESNA Conference, Washington, DC, 1990, pp. 173–174.